HHS Public Access

Author manuscript

Soft Matter. Author manuscript; available in PMC 2017 September 13.

Published in final edited form as:

Soft Matter. 2016 September 13; 12(36): 7521–7528. doi:10.1039/c6sm01349j.

Membrane Mechanical Properties of Synthetic Asymmetric Phospholipid Vesicles

Li Lu[1,3], **William J. Doak**[1], **Jeffrey W. Schertzer**[2,3], and **Paul R. Chiarot**[1,3]

Paul R. Chiarot: pchiarot@binghamton.edu

[1]Department of Mechanical Engineering, State University of New York at Binghamton, Binghamton, NY, USA

[2]Department of Biological Sciences, State University of New York at Binghamton, Binghamton, NY, USA

[3]Binghamton Biofilm Research Center, State University of New York at Binghamton, Binghamton, NY, USA

Abstract

Synthetic lipid vesicles have served as important model systems to study cellular membrane biology. Research has shown that the mechanical properties of bilayer membranes significantly affects their biological behavior. The properties of a lipid bilayer are governed by lipid acyl chain length, headgroup type, and the presence of membrane proteins. However, few studies have explored how membrane architecture, in particular trans-bilayer lipid asymmetry, influences membrane mechanical properties. In this study, we investigated the effects of lipid bilayer architecture (i.e. asymmetry) on the mechanical properties of biological membranes. This was achieved using a customized micropipette aspiration system and a novel microfluidic technique previously developed by our team for building asymmetric phospholipid vesicles with tailored bilayer architecture. We found that the bending modulus and area expansion modulus of the synthetic asymmetric bilayers were up to 50% larger than the values acquired for symmetric bilayers. This was caused by the dissimilar lipid distribution in each leaflet of the bilayer for the asymmetric membrane. To the best of our knowledge, this is the first report on the impact of trans-bilayer asymmetry on the area expansion modulus of synthetic bilayer membranes. Since the mechanical properties of bilayer membranes play an important role in numerous cellular processes, these results have significant implications for membrane biology studies.

INTRODUCTION

Synthetic lipid vesicles are spherical structures comprised of a single lipid bilayer (i.e. membrane) surrounding an aqueous lumen. Lipid bilayers are mimics of naturally occurring cellular membranes and have served as stable model systems to investigate many biological processes, including: the behavior of membrane proteins (e.g. folding and gating),[1–4] lipid-protein interactions,[5] mechanism of cell endocytosis and membrane vesicle budding,[6,7] and morphological changes of the membrane.[8] Most of these biological processes are heavily influenced by the mechanical properties of the cell membrane, where even small changes are critical to these highly specific membrane functions. This leads to an increasing need to understand the relationship between the bilayer membrane architecture and its mechanical

properties, especially the bending modulus (i.e. representing the energy required to deform a flat surface into a curved structure) and membrane area expansion modulus (i.e. representing the membrane resistance to isotropic area expansion). Synthetic vesicles are a useful tool to explore this question.

It has been reported that the mechanical properties of a bilayer membrane are significantly affected by the lipid fatty acyl chain length,[9,10] headgroup type,[11] and the presence of membrane proteins.[12] However, few studies have investigated the effect of *trans-bilayer lipid asymmetry* on membrane mechanical properties. In nature, all cellular membranes possess some degree of lipid asymmetry across the bilayer. That is, the composition of one leaflet is different from the other leaflet. The degree of asymmetry can vary, from subtle differences in the distribution of certain phospholipids in eukaryotic membranes to the outer membrane of Gram-negative bacteria, which are believed to be almost completely asymmetric between two widely different lipid types.[13–15] This added complexity has been found to have important consequences for the bending modulus of lipid bilayers that are assembled into giant unilamellar vesicles (GUVs) constructed using emulsion phase transfer techniques.[16,17] However, to our knowledge, the influence of trans-bilayer membrane asymmetry on area expansion modulus has not been previously investigated.

Over the last few decades, some of the most widely adopted vesicle preparation techniques include extrusion,[18] electroformation,[19] and hydration.[20] These conventional techniques enable the large-scale production of vesicles, but often lead to non-uniform vesicle sizes and non-unilamellar membranes. This issue has been largely overcome by the introduction of microfluidic technology to vesicle preparation techniques,[21,22] including hydrodynamic flow focusing,[23] pulsed jetting,[24,25] aqueous emulsion transfer,[26–28] and oil phase removal from double emulsions.[29–31] However, these methods lack control over the trans-bilayer lipid distribution (i.e. the membrane architecture) and they typically result in a symmetric bilayer with identical lipid composition in each leaflet. To build vesicles with trans-bilayer asymmetry, several approaches have emerged in recent years, such as reverse and microfluidic-modified reverse emulsification,[32–34] donor-acceptor lipid exchange,[35] and layer-by-layer assembly.[36] These approaches suffered from some limitations, including vesicle size variation, limited vesicle throughput, restriction to only single cell studies, and difficulty in transferring the vesicles off-chip. Therefore, an innovative strategy was needed to address the inability of these methods to build asymmetric vesicles at high-throughput while simultaneously controlling membrane unilamellarity, vesicle size, monodispersity, and luminal content. In our previous work, we developed a continuous microfluidic fabrication strategy to solve this issue.[37] This strategy first builds monodisperse water-in-oil emulsions to serve as templates where the inner-leaflet of the synthetic vesicles assemble at the emulsion interface. To achieve membrane asymmetry, the next step is to replace the lipids in the oil phase with the outer-leaflet lipids. Lastly, water-in-oil-in-water double emulsions are produced and the outer-leaflet is assembled to create a customized bilayer after an oil extraction process. This strategy offers a flexible and reliable way to continuously build monodisperse GUVs with tailored membrane composition, while providing simultaneous control over membrane unilamellarity, vesicle size, and luminal content. Trans-bilayer asymmetry and unilamellarity of the GUVs is confirmed using fluorescence-quenching assays.[37] This strategy for building synthetic vesicles is an essential tool for investigating the

effects of trans-bilayer asymmetry on the mechanical properties of biologically relevant membranes.

Several techniques have been developed to measure the mechanical properties of biological membranes, including: fluctuation spectroscopy,[38] dynamic light scattering,[39] and nuclear magnetic resonance and X-ray diffraction.[40] However, the most widely used technique for accurate and direct measurement of a single membrane system is micropipette aspiration. It is an *in situ*, invasive method, where a small part of the membrane is aspirated by a glass micropipette with a known suction pressure. The tension acting on the entire membrane is proportional to the applied suction. With increasing membrane tension, the aspiration length increases and leads to a proportional change of the total area of the membrane. By using the geometric conditions and measured values of the suction pressure and aspiration length, the membrane mechanical properties such as area expansion (i.e. dialation),[41,42] shear,[43] and bending moduli,[44,45] as well as membrane surface viscosity and interlayer friction,[46,47] can be calculated. In practice, micropipette aspiration has proven useful in studying the physical properties of symmetric biological membranes. For example, when applied to large unilamellar vesicles, it provided detailed information on how the symmetric bilayer content affects the rupture tension and water permeability,[48] as well as the phase behavior over a wide range of sterol concentrations.[49] In addition, it has also enabled the study of the material properties of polymersomes,[50] the adsorption of small molecules into the bilayer,[51] and the interfacial tension of microscopic lipid monolayers.[52]

In this work, we investigated the effects of trans-bilayer membrane asymmetry on the mechanical properties of lipid bilayers of GUVs using our novel microfluidic vesicle fabrication strategy and the micropipette aspiration technique. We confirmed that symmetric GUVs produced using our strategy had similar mechanical properties to those formed via conventional preparation methods. Significantly, we obtain the first measurements showing that an important membrane mechanical property, the area expansion modulus, is heavily influenced by the architecture (i.e. the asymmetry) of the synthetic lipid bilayer. In the following sections, we describe our methodologies for building GUVs using our continuous microfluidic fabrication strategy, fabricating micropipettes, and operating our customized hydrostatic pressure system. We then report on our micropipette aspiration experiments and measurements of area expansion and bending moduli.

MATERIALS AND METHODS

Chemicals

1,2-dioleoyl-sn-glycero-3-phosphocholine (DOPC) and 1,2-dimyristoyl-sn-glycero-3-phosphocholine (DMPC) were purchased from Avanti Polar Lipids (25 mg/ml in chloroform). NBD labeled phosphocholine, 2-(12-(7-nitrobenz-2-oxa-1,3-diazol-4-yl)amino)dodecanoyl-1-hexadecanoyl-sn-glycero-3-phosphocholine (NBD-PC) was obtained from Life Technologies. Polydimethylsiloxane (PDMS) prepolymer and curing agent kits (Sylgard 184) were purchased from Ellsworth Adhesives. Sodium dithionite (fluorescence quencher for NBD-PC) and α-hemolysin were obtained from Sigma-Aldrich. All other chemicals, including oleic acid, glucose, and sucrose were purchased from VWR.

Vesicle Preparation

When preparing vesicles synthetically at high-throughput, it is difficult to simultaneously control the vesicle size and uniformity and the membrane asymmetry and unilamellarity. In this work, giant unilamellar vesicles were built using our previously developed continuous on-chip fabrication strategy.[37,53] This strategy uses a customized PDMS microfluidic device on which monodisperse symmetric or asymmetric vesicles with tailored membrane composition, size, and luminal content are built at high-throughput. The microchannels of the microfluidic device consist of a triangular post region and two flow-focusing regions, where the following steps are performed to build the GUVs: (1) inner-leaflet assembly on w/o emulsions templates formed at the first flow-focusing region, (2) replacement of the inner-leaflet-lipid with the outer-leaflet-lipid in the oil phase using a continuous hydrodynamic flow separation technique in the triangular post region,[54,55] (3) outer-leaflet assembly on w/o/w double emulsions formed at the second flow-focusing region, and (4) extraction of the intermediate oil layer from the double emulsions. Oleic acid was used as the oil phase to carry the lipids. Glucose (0.2 M) was added to the inner aqueous phase in order to balance the osmolarity with the outer aqueous phase (i.e. containing 0.2 M sucrose) while maintaining a density difference. This strategy has a high yield of GUVs with a controllable radius (10 ~ 130 μm), and over 80% of the GUVs remain stable for at least 6 weeks at room temperature.

Five types of GUVs were built using DMPC and DOPC for this study, including three types of symmetric vesicles and two types of asymmetric vesicles (depicted in Fig. 1). Note that we categorize the GUVs made of mixed DOPC and DMPC (1:1) lipids as symmetric vesicles, even though the exact local trans-bilayer lipid distribution may be asymmetric. Membrane asymmetry and unilamellarity were confirmed using two assays we previously developed.[37] Membrane asymmetry was confirmed using a fluorescence-quenching assay for NBD labeled lipids that were added to one leaflet of the GUV membrane. This assay showed that immediately after formation, membrane asymmetry as high as 95% was achieved. The asymmetry was maintained at a high-degree for over 30 hours. Membrane unilamellarity was confirmed by inserting proteins (α-hemolysins) into the GUV bilayer and verifying the formation of transmembrane pores.

Micropipette Fabrication

The mechanical properties of the synthetic vesicles were measured using suction pressure provided by a micropipette. The micropipettes were made from borosilicate glass capillaries (1 mm in O.D., World Precision Instrument) that were pulled (Sutter Instrument) to the desired tip diameter. The typical inner diameter was ~20μm. Our experiments required micropipettes with cleanly broken tips that remain cylindrical for at least the length of the aspirated membrane. In practice, this can be achieved using different methods (e.g. microforging);[56,57] however, our preferred technique used a customized pipette cutter that made cleanly broken tips with the desired diameter.

Micropipette Aspiration Measurement

The membrane mechanical properties were measured using a custom-designed hydrostatic pressure system (as illustrated in Fig. 2), an inverted microscope (Leica), and a

micromanipulator to position the micropipette. A CCD camera (Qimaging) connected to the microscope was used for image capture. The hydrostatic pressure system monitored the suction pressure applied to the vesicles through the micropipette. This system includes a linear translational stage (part c, from Edmund Optics) mounted vertically to the side of an optical table. This stage shifts two identical plexiglass water reservoirs (part a and b, ~100 mL each) with ports on the top and bottom to a defined height relative to the opening of the micropipette. One of the water reservoirs (part a) is attached to a second linear stage (part d), allowing for a total vertical difference in height of up to 55 cm between the two reservoirs. This creates a pressure difference between the two reservoirs. Tubing (C-flex, Cole-Parmer) connects from the bottom port of each reservoir (through stop valves e and f) to a low-pressure differential transducer (part h, OMEGA PX2300) to measure the static pressure difference between the reservoirs. The output of the transducer was monitored using a digital multimeter. The accuracy of the measured pressure was confirmed by recording the travel distance of the reservoir (part a) and calculating the change in pressure. A separate section of tubing connects the water reservoirs through a stop valve (part g). Tubing (PTFE, Cole-Parmer) connects the reservoir (part a) to the micropipette through a connection fitting (part i, IDEX, PEEK). The fitting is mounted on the three-axis micromanipulator (Tektronix) to precisely control the position of the micropipette. We selectively closed the valves (part e and f) to install the transducer and took extreme care to expel all air bubbles from the system before measurements were taken. In addition, we kept the system under slight positive pressure when not in use. Equilibration of the water level in the two reservoirs was achieved by opening the stop valve (part g). This valve must remain closed during the pressure measurements while the other valves (part e and f) remain open.

The micropipette was immersed in a vesicle sample holder (part j) made of PDMS and filled with 1 mL of a GUV suspension. The wall of the sample holder was low to minimize the angle between the pipette and the bottom of the holder. A customized, transparent plastic cover was used to reduce the evaporation of water and the corresponding change in concentration of the vesicle suspension. A small slot was made on the side of the plastic cover to allow for manipulation of the micropipette. The zero pressure position in the micropipette was determined by sucking small latex microspheres (2 μm in mean particle size, Sigma-Aldrich) into the pipette and stopping their movement in the pipette by adjusting the height of both reservoirs (part c). After setting the zero pressure point, the micropipette was brought into contact with a GUV. One reservoir was then lowered (part d) to create a pressure difference between the two reservoirs, which was equal to the pressure applied to the GUV. With increasing suction pressure, the aspiration length in the micropipette increased until the vesicle ruptured. The hydrostatic pressure system provides a suction pressure of up to 540 Pa with a resolution of 0.1 Pa when using water.

All experiments were carried out at 22.5°C. We used ImageJ for image processing and measurements. After each pressure increment, we waited for 5 seconds before taking measurements (i.e. to ensure the system reached equilibrium). Micropipette radius, vesicle radius, and the aspiration length (ΔL, from the entrance of the pipette to the end of the vesicle projection) at each applied suction pressure value were recorded to calculate the bending modulus and membrane area expansion modulus (Fig. 3).

THEORETICAL CONSIDERATIONS

Bending modulus and membrane area expansion modulus of the GUVs were measured using the micropipette aspiration technique and followed the theoretical analysis developed by Evans *et al.*[9,45,58] Upon aspiration of a portion of the vesicle membrane, the induced isotropic membrane tension (τ) is related to the applied suction pressure (ΔP) as:

$$\tau = \frac{\Delta P R_P}{2(1 - \frac{R_P}{R_V})} \quad (1)$$

where R_P and R_V denote the pipette and the vesicle radii, respectively (see Fig. 3a). As ΔP is gradually increased, the aspiration length (ΔL) increases due to the membrane's elastic response to the mechanical stress. According to Evans *et al.*, ΔL is related to the observed apparent area strain (α_{app}) as:

$$\alpha_{app} = \frac{\Delta A}{A_0} = \frac{2\pi R_P \Delta L}{A_0}\left(1 - \frac{R_P}{R_V}\right) = \frac{\Delta L[(R_P/R_V)^2 - (R_P/R_V)^3]}{2R_P} \quad (2)$$

where A_0 is the membrane area of the GUV measured at an initial low tension state and A is the membrane area after pressurization to a higher tension state. In the low-tension regime (<0.5 mN/m), the lipid bilayer is assumed to be incompressible, thus the total membrane area is constant. However, there is a loss of configurational entropy for the lipid molecules due to smoothing of the thermal undulations. This leads to an optically resolvable increase in the relative change of α_{app} (Fig. 4a). It has been shown that the product of the bending modulus (κ) and α_{app} is proportional to the natural logarithm of membrane tension:

$$\ln\frac{\tau}{\tau_0} = \left(\frac{8\pi\kappa}{k_B T}\right)\alpha_{app} \quad (3)$$

where k_B is the Boltzmann constant and T is the absolute temperature. The bending modulus, κ, is determined by plotting $\ln(\tau)$ vs α_{app} in the tension range up to 0.5 mN/m and taking the product of the slope with $k_B T/8\pi$. The plot of $\ln(\tau)$ vs α_{app} for an asymmetric DOPC-DMPC GUV is shown in Fig. 4b (blue curve). In the high-tension regime (>0.5 mN/m), the membrane is strained due to the direct expansion of the area per molecule (Fig. 4a). Thus, α_{app} is governed by the membrane area expansion and increases linearly with tension (red curve in Fig. 4b):

$$\tau = K_{app}\alpha_{app} \quad (4)$$

By convention, the slope is known as the apparent area expansion modulus (K_{app}). The direct area expansion modulus (K_{dir}) is determined by subtracting the logarithmic contribution from α_{app} (for each i-th value) to get the direct area strain (α_{dir}):

$$\alpha_{\mathrm{dir}}(i)=\alpha_{\mathrm{app}}(i)-\Delta\alpha(i)=\alpha_{\mathrm{app}}(i)-\left(\frac{k_BT}{8\pi\kappa_{\mathrm{avg}}}\right)\ln\left(\frac{\tau_{(i)}}{\tau_{(1)}}\right) \quad (5)$$

where κ_{avg} is the average bending modulus and $\tau_{(1)}$ is the initial tension state of the high tension regime (set at 0.75 mN/m in this study). K_{dir} is the revised slope for plotting τ vs α_{dir} (black curve in Fig. 4b):

$$\tau=K_{\mathrm{dir}}\alpha_{\mathrm{dir}} \quad (6)$$

RESULTS

The micropipette aspiration technique yields direct information on the bending modulus (κ) and the direct area expansion modulus (K_{dir}) of the GUVs. The membrane tension induced by suction increases with the relative area expansion of the whole vesicle. In the low-tension regime, the area expansion is dominated by smoothing of membrane thermal undulations, which is indicated by the linear dependence of membrane area strain on the logarithm of membrane tension (Eq. 3). In the high-tension regime, the area expansion is mainly influenced by the membrane area expansion modulus, which results in a linear dependence of tension on area expansion (Eq. 6). We performed measurements on GUVs with five different lipid compositions: symmetric vesicles with two different one-component compositions (DMPC and DOPC), symmetric vesicles with two-component composition (DMPC/DOPC at 1:1 mixture), and two asymmetric vesicles with two-component compositions (DMPC or DOPC on the inner leaflet and DOPC or DMPC on the outer leaflet). We chose DMPC and DOPC lipids to build the vesicles because their κ and K_{dir} values have been reported in the literature for symmetric GUVs made using conventional vesicle preparation techniques (e.g. electroformation).[59,60] In addition, it has been found that there is no significant difference in the mechanical properties of vesicle membranes prepared by these conventional methods and the droplet microfluidics-based approaches.[16,61] Thus, the values reported in the literature can be used to verify our experiment results for the symmetric vesicles. Measurements were performed on at least eight vesicles for each type of GUV and the complete results are listed in Table 1.

Bending moduli of the symmetric DMPC and DOPC vesicles were found to be (11.8 ± 1.3) × 10^{-20} J and (9.1 ± 1.5) × 10^{-20} J, respectively (all values are given as mean ± SD). Their direct area expansion moduli were found to be 173 ± 20 mN/m and 210 ± 25 mN/m, respectively. The results (measured at T = 22.5°C) follow the trends of previously reported values for symmetric DOPC and DMPC vesicles.[9,59,60] It is worth noting that both bending and area expansion moduli for the DMPC bilayer reach their minimum values when approaching the fluid-gel main transition temperature ($T_m \cong 23.4$°C).[62,63] At this temperature, the bilayer consists of mixed fluid-state and gel-states lipids leading to the formation of periodic membrane ripples.[64,65] This result highlights the accuracy of our hydrostatic pressure system in measuring the elastic properties of GUVs produced by our microfluidic fabrication strategy. The bending modulus and direct area expansion modulus

of symmetric GUVs (with DMPC/DOPC at 1:1 mixture) were measured to be (11.2 ± 1.4) × 10^{-20} J and 182 ± 15 mN/m, similar to the single component systems.

Most importantly, we found that the lipid distribution strongly influences the mechanical properties of the bilayer for asymmetric vesicles compared to symmetric vesicles. The bending moduli of the asymmetric GUVs (Inner: DMPC - Outer: DOPC) and (Inner: DOPC - Outer: DMPC) were found to be (17.2 ± 2.5) × 10^{-20} J and (16.8 ± 2.1) × 10^{-20} J, respectively. Their direct area expansion moduli were found to be 248 ± 20 mN/m and 254 ± 19 mN/m, respectively. Therefore, the mean values of both the bending and area expansion moduli of the asymmetric bilayers are larger than the values for their symmetric counterparts. The two-tailed *t*-test was used to determine if the difference in the mean values of the bending and area expansion moduli between the symmetric and asymmetric GUVs were statistically significant. When comparing κ and K_{dir} for the asymmetric vesicles against each of the symmetric vesicles, the P-values were less than 0.005 in all cases. This highlights that the measured differences in the mean value of κ and K_{dir} were always statistically significant when comparing the asymmetric to symmetric vesicles. The values of the bending modulus of the asymmetric bilayers are about 50% higher than that of the symmetric ones. A similar relationship has been reported in the literature.[16,17] The results also show that there is no significant difference in the moduli between the two asymmetric bilayer compositions (P-values > 0.5).

We believe there may be several rationales for the change in bilayer membrane mechanical properties due to the introduction of trans-bilayer asymmetry in the GUVs. First, bending modulus represents the energetic penalty in deforming a flat bilayer into a curved one. The curvature elastic energy per unit area of the bilayer was found to be strongly dependent on the spontaneous curvature and bending modulus of each monolayer.[66] In a symmetric bilayer, we only consider the values of a single lipid monolayer (even in a two-component symmetric system). However, in an asymmetric bilayer, we need to consider the bilayer as two individual monolayers with independent spontaneous curvature and bending modulus values.[67,68] This is because each lipid shape that deviates from a cylinder (i.e. packing factor deviating from unity) contributes to the spontaneous curvature of the monolayer. In this study, DOPC and DMPC have different spontaneous curvatures and bending moduli. If we assume the bilayer as being made of two parallel (flat) monolayers with constant overall bilayer composition - but varying distribution of lipids between the two monolayers - its curvature elastic energy (per unit area) reaches a minimum when the bilayer becomes symmetric.[17] This conclusion suggests that a symmetric bilayer is at a lower energy state compared to an asymmetric bilayer and is consistent with our measurement of bending modulus.

Second, the membrane area expansion modulus represents the membrane's resistance to isotropic area expansion. The resistant forces may be due to hydrophobic interactions between coupled lipid molecules (on different leaflets) and/or neighboring lipids (on the same leaflet). The higher area expansion modulus of an asymmetric versus symmetric system indicates that the two systems have different membrane expansion properties due to dissimilar lipid distributions. This can be explained by considering the fact that DMPC (diC14:0) has shorter acyl chain length than DOPC (diC18:1). Therefore, in a DMPC/DOPC

(1:1 mixture) symmetric bilayer, due to the mismatch between longer-chain lipid pairs and shorter-chain lipid pairs, the extra free space[69] available to the longer chains (i.e. DOPC chains) near the bilayer mid-plane would largely weaken the bilayer, thus reducing the area expansion modulus compared to that of their asymmetric counterparts.[10,70] A similar configuration may also apply to the DMPC symmetric bilayer, where the lipids are in a fluid-gel mixture state, and the fluid lipids would have shorter chain lengths than the gel lipids.[65,71] Our results also indicate that, compared to a DOPC symmetric bilayer, the asymmetric DMPC-DOPC bilayers have higher area expansion moduli, which may result from the introduction of gel-state lipids (DMPC) to fluid-state lipids (DOPC) that strengthens the bilayer's resistance to expansion. This offers an explanation as to why an asymmetric bilayer has a higher area expansion modulus compared to a symmetric bilayer and is consistent with our measurements.

SUMMARY

In this work, we investigated the effects of trans-bilayer asymmetry on the mechanical properties of lipid bilayers by combining our novel microfluidic vesicle fabrication strategy and the micropipette aspiration technique. We measured the bending and area expansion moduli of five types of GUVs made of DMPC and DOPC, including three types of symmetric and two types of asymmetric GUVs. We found that both the bending and area expansion moduli of asymmetric bilayers are larger than the values of symmetric bilayers. The results for bending moduli are in close agreement with literature values, thus confirming the GUVs produced using our strategy have similar mechanical properties to those formed via other conventional preparation methods. In addition, we proposed an explanation as to why the symmetric bilayers (DMPC/DOPC at 1:1 mixture) have a lower area expansion modulus than the asymmetric bilayers. Specifically, the mismatch between different lipid tails creates extra free space for the longer tails near the bilayer mid-plane that largely weakens the symmetric bilayer.

The fundamental mechanical properties of bilayer membranes play an important role in many cellular processes and have significant implications for membrane biology studies, including: (i) protein-lipid interactions of integral membrane proteins (e.g. the gating mechanism of mechanosensitive channels is found to be controlled by trans-bilayer asymmetry of the lateral pressure profile);[3,72] (ii) membrane protein folding rate (e.g. increasing bending modulus of the bilayer is found to slow the rate of formation of the partially folded apoprotein intermediate);[4] (iii) membrane lipid synthesis, which is strongly influenced by the lipid arrangement in the bilayer and regulated by bending modulus;[73] (iv) morphology of large unilamellar vesicles, which is influenced by bilayer asymmetry and its minimum membrane bending energy;[74] and (v) the ability of cell membranes to deform during endo- and exocytosis,[67] bacterial outer membrane vesicle formation,[75] and osmotic swelling where the membrane is strained and resistant to osmotic stress.[70] Therefore, our strategy for building and evaluating asymmetric GUVs with tailored bilayer membrane architectures paves the way for studies in all of these areas. To expand our knowledge of the precise role that trans-bilayer asymmetry plays in cellular membranes, further studies are needed to measure the mechanical properties of GUVs made of other types of lipids and different trans-bilayer compositions.

Supplementary Material

Refer to Web version on PubMed Central for supplementary material.

Acknowledgments

This research was supported by the National Science Foundation (DBI Award #1429448) and the National Institute of Allergy and Infectious Diseases (1R21AI121848-01). Our thanks to Sepehr Maktabi (State University of New York at Binghamton) for enlightening discussions.

REFERENCES

1. Jesorka A, Orwar O. Annu. Rev. Anal. Chem. 2008; 1:801–832.
2. Lasic DD. Trends Biotechnol. 1998; 16:307–321. [PubMed: 9675915]
3. Perozo E, Kloda A, Cortes DM, Martinac B. Nat. Struct. Mol. Biol. 2002; 9:696–703.
4. Booth PJ, Riley ML, Flitsch SL, Templer RH, Farooq A, Curran AR, Wright P. Biochemistry. 1997; 36:197–203. [PubMed: 8993334]
5. Gómez-Hens A, Fernández-Romero JM. Trends Analyt. Chem. 2005; 24:9–19.
6. Pomorski T, Lombardi R, Riezman H, Devaux PF, van Meer G, Holthuis JC. Mol. Biol. Cell. 2003; 14:1240–1254. [PubMed: 12631737]
7. Daleke DL. J. Biol. Chem. 2007; 282:821–825. [PubMed: 17130120]
8. Bloom M, Evans E, Mouritsen OG. Q. Rev. Biophys. 1991; 24:293–397. [PubMed: 1749824]
9. Rawicz W, Olbrich KC, McIntosh T, Needham D, Evans E. Biophys. J. 2000; 79:328–339. [PubMed: 10866959]
10. Ali S, Smaby JM, Momsen MM, Brockman HL, Brown RE. Biophys. J. 1998; 74:338–348. [PubMed: 9449334]
11. Brüning B, Stehle R, Falus P, Farago B. Eur. Phys. J. E. 2013; 36:1–8. [PubMed: 23306446]
12. Girard P, Prost J, Bassereau P. Phys. Rev. Lett. 2005; 94:088102. [PubMed: 15783939]
13. Bretscher MS. J. Mol. Biol. 1972; 71:523–528. [PubMed: 4648341]
14. Zachowski A. Biochem. J. 1993; 294:1. [PubMed: 8363559]
15. Kamio Y, Nikaido H. Biochemistry. 1976; 15:2561–2570. [PubMed: 820368]
16. Karamdad K, Law RV, Seddon JM, Brooks NJ, Ces O. Chem. Commun. 2016; 52:5277–5280.
17. Elani Y, Purushothaman S, Booth PJ, Seddon JM, Brooks NJ, Law RV, Ces O. Chem. Commun. 2015; 51:6976–6979.
18. Olson F, Hunt CA, Szoka FC, Vail WJ, Papahadjopoulos D. Biochim. Biophys. Acta, Biomembr. 1979; 557:9–23.
19. Angelova MI, Dimitrov DS. Faraday Discuss. Chem. Soc. 1986; 81:303–311.
20. Hishida M, Seto H, Yamada NL, Yoshikawa K. Chem. Phys. Lett. 2008; 455:297–302.
21. Swaay DV, deMello A. Lab Chip. 2013; 13:752–767. [PubMed: 23291662]
22. Capretto L, Carugo D, Mazzitelli S, Nastruzzi C, Zhang X. Adv. Drug Delivery Rev. 2013; 65:1496–1532.
23. Jahn A, Vreeland WN, Gaitan M, Locascio LE. J. Am. Chem. Soc. 2004; 126:2674–2675. [PubMed: 14995164]
24. Funakoshi K, Suzuki H, Takeuchi S. J. Am. Chem. Soc. 2007; 129:12608–12609. [PubMed: 17915869]
25. Stachowiak JC, Richmond DL, Li TH, Liu AP, Parekh SH, Fletcher DA. Proc. Natl. Acad. Sci. U. S. A. 2008; 105:4697–4702. [PubMed: 18353990]
26. Noireaux V, Libchaber A. Proc. Natl. Acad. Sci. U. S. A. 2004; 101:17669–17674. [PubMed: 15591347]
27. Ota S, Yoshizawa S, Takeuchi S. Angew. Chem., Int. Ed. 2009; 48:6533–6537.
28. Matosevic S, Paegel BM. J. Am. Chem. Soc. 2011; 133:2798–2800. [PubMed: 21309555]

29. Tan YC, Hettiarachchi K, Siu M, Pan YR, Lee AP. J. Am. Chem. Soc. 2006; 128:5656–5658. [PubMed: 16637631]
30. Shum HC, Lee D, Yoon I, Kodger T, Weitz DA. Langmuir. 2008; 24:7651–7653. [PubMed: 18613709]
31. Arriaga LR, Datta SS, Kim SH, Amstad E, Kodger TE, Monroy F, Weitz DA. Small. 2014; 10:950–956. [PubMed: 24150883]
32. Pautot S, Frisken BJ, Weitz DA. Proc. Natl. Acad. Sci. U. S. A. 2003; 100:10718–10721. [PubMed: 12963816]
33. Hamada T, Miura Y, Komatsu Y, Kishimoto Y, Vestergaard M, Takagi M. J. Phys. Chem. B. 2008; 112:14678–14681. [PubMed: 18983183]
34. Hu PC, Li S, Malmstadt N. ACS Appl. Mater. Interfaces. 2011; 3:1434–1440. [PubMed: 21449588]
35. Cheng HT, Megha, London E. J. Biol. Chem. 2009; 284:6079–6092. [PubMed: 19129198]
36. Matosevic S, Paegel BM. Nat. Chem. 2013; 5:958–963. [PubMed: 24153375]
37. Lu L, Schertzer JW, Chiarot PR. Lab Chip. 2015; 15:3591–3599. [PubMed: 26220822]
38. Schneider MB, Jenkins JT, Webb WW. J. Phys. 1984; 45:1457–1472.
39. Hallett FR, Marsh J, Nickel BG, Wood JM. Biophys. J. 1993; 64:435. [PubMed: 8457669]
40. Koenig BW, Strey HH, Gawrisch K. Biophys. J. 1997; 73:1954. [PubMed: 9336191]
41. Evans E, Needham DJ. Phys. Chem. 1987; 91:4219–4228.
42. Kwok R, Evans E. Biophys. J. 1981; 35:637–652. [PubMed: 7272454]
43. Waugh R, Evans EA. Biophys. J. 1979; 26:115–131. [PubMed: 262408]
44. Bo L, Waugh RE. Biophys. J. 1989; 55:509–517. [PubMed: 2930831]
45. Evans E, Rawicz W. Phys. Rev. Lett. 1990; 64:2094–2097. [PubMed: 10041575]
46. Hochmuth RM, Wiles HC, Evans EA, McCown JT. Biophys. J. 1982; 39:83–89. [PubMed: 7104454]
47. Evans E, Yeung A. Chem. Phys. Lipids. 1994; 73:39–56.
48. Olbrich K, Rawicz W, Needham D, Evans E. Biophys. J. 2000; 79:321–327. [PubMed: 10866958]
49. Tierney KJ, Block DE, Longo ML. Biophys. J. 2005; 89:2481–2493. [PubMed: 16055540]
50. Mabrouk E, Cuvelier D, Pontani LL, Xu B, Lévy D, Keller P, Li MH. Soft Matter. 2009; 5:1870–1878.
51. Ly HV, Longo ML. Biophys. J. 2004; 87:1013–1033. [PubMed: 15298907]
52. Lee S, Kim DH, Needham D. Langmuir. 2001; 17:5544–5550.
53. Lu, L.; Schertzer, JW.; Chiarot, PR. presented in part at the ASME 2015 13th International Conference on Nanochannels, Microchannels, and Minichannels; July 2015; San Francisco.
54. Lu L, Irwin RM, Coloma MA, Schertzer JW, Chiarot PR. Microfluid. Nanofluid. 2015; 18:1233–1246.
55. Lu, L.; Irwin, RM.; Schertzer, JW.; Chiarot, PR. presented in part at the ASME 2014 International Mechanical Engineering Congress and Exposition; November 2014; Montreal.
56. Longo ML, Ly HV. Methods Mol. Biol. 2007; 400:421–437. [PubMed: 17951750]
57. Heinrich V, Rawicz W. Langmuir. 2005; 21:1962–1971. [PubMed: 15723496]
58. Evans E, Needham D. J. Phys. Chem. 1987; 91:4219–4228.
59. Meleard P, Gerbeaud C, Pott T, Fernandez-Puente L, Bivas I, Mitov MD, Bothorel P. Biophys. J. 1997; 72:2616. [PubMed: 9168037]
60. Gracià RS, Bezlyepkina N, Knorr RL, Lipowsky R, Dimova R. Soft Matter. 2010; 6:1472–1482.
61. Karamdad K, Law RV, Seddon JM, Brooks NJ, Ces O. Lab Chip. 2015; 15:557–562. [PubMed: 25413588]
62. Evans E, Kwok R. Biochemistry. 1982; 21:4874–4879. [PubMed: 7138837]
63. Dimova R, Pouligny B, Dietrich C. Biophys. J. 2000; 79:340–356. [PubMed: 10866960]
64. Needham D, Evans E. Biochemistry. 1988; 27:8261–8269. [PubMed: 3233209]
65. Heimburg T. Biophys. J. 2000; 78:1154–1165. [PubMed: 10692305]
66. Helfrich W. Z. Naturforsch. C Bio. Sci. 1973; 28:693–703.

67. Brooks NJ, Ces O, Templer RH, Seddon JM. Chem. Phys. Lipids. 2011; 164:89–98. [PubMed: 21172328]
68. Kollmitzer B, Heftberger P, Rappolt M, Pabst G. Soft Matter. 2013; 9:10877–10884. [PubMed: 24672578]
69. Illya G, Lipowsky R, Shillcock JC. J. Chem. Phys. 2005; 122:244901. [PubMed: 16035810]
70. Janmey PA, Kinnunen PKJ. Trends Cell Biol. 2006; 16:538–546. [PubMed: 16962778]
71. Heimburg T. Biochim. Biophys. Acta. 1998; 1415:147–162. [PubMed: 9858715]
72. Chang G, Spencer RH, Lee AT, Barclay MT, Rees DC. Science. 1998; 282:2220–2226. [PubMed: 9856938]
73. Attard GS, Templer RH, Smith WS, Hunt AN, Jackowski S. Proc. Natl. Acad. Sci. U. S. A. 2000; 97:9032–9036. [PubMed: 10908674]
74. Mui BL, Döbereiner HG, Madden TD, Cullis PR. Biophys. J. 1995; 69:930. [PubMed: 8519993]
75. Schertzer JW, Whiteley M. mBio. 2012; 3 e00297-11.

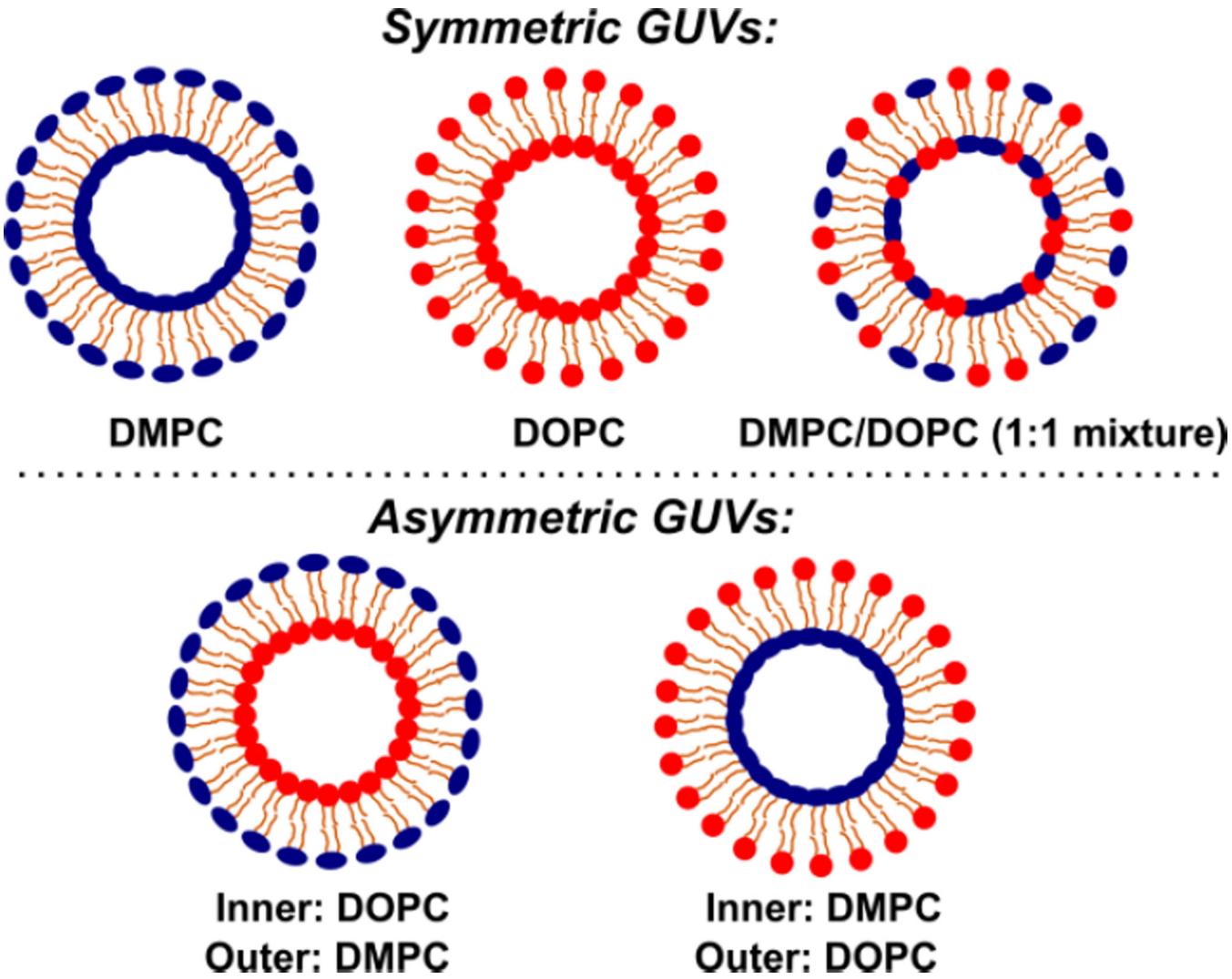

Figure 1.

Schematics of five types of giant unilamellar vesicles (GUVs) with different lipid compositions, including three symmetric GUVs made of DMPC, DOPC, and DMPC/DOPC (1:1 mixture), respectively, and two asymmetric GUVs made of DMPC (or DOPC) on the inner leaflet and DOPC (or DMPC) on the outer leaflet. We have created synthetic GUVs with trans-bilayer asymmetries as high as 95%.[37]

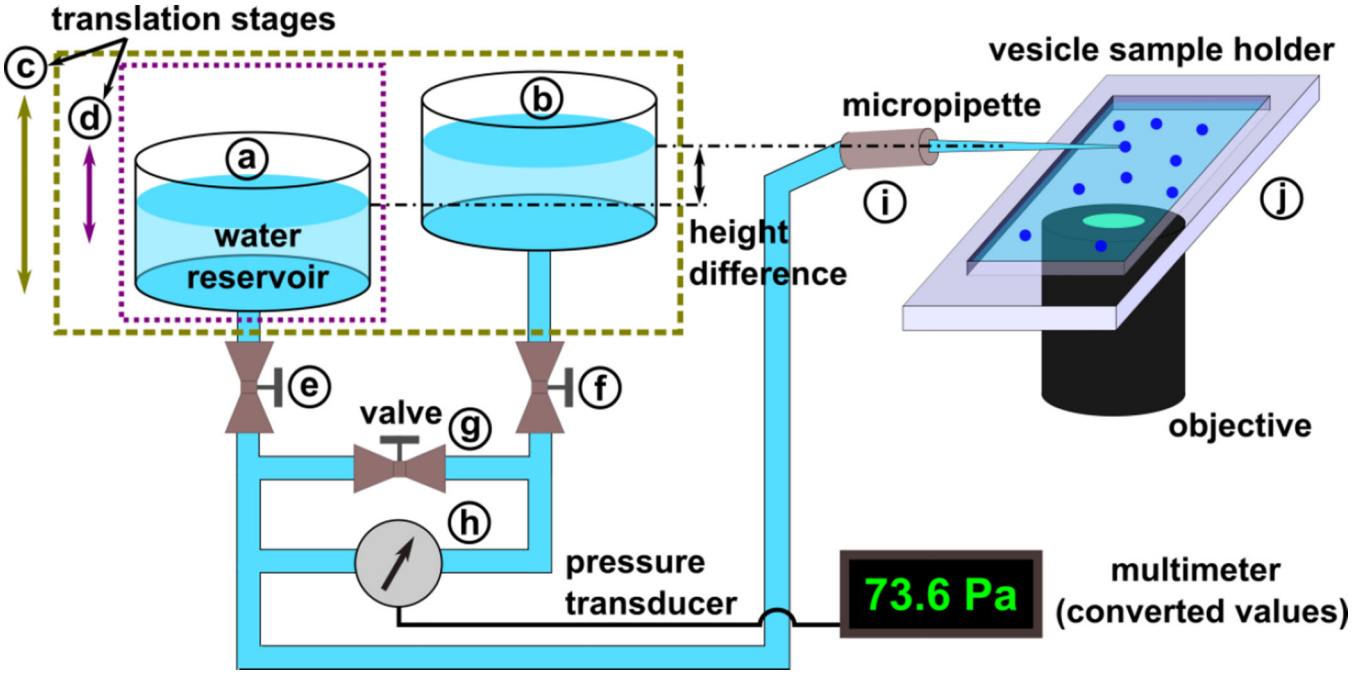

Figure 2.

Schematic representation of a customized hydrostatic pressure system: (a, b) water reservoir, (c, d) linear translation stage, (e, f, g) two-way stop valve, (h) low differential pressure transducer, (i) micropipette connection fitting, and (j) PDMS sample holder.

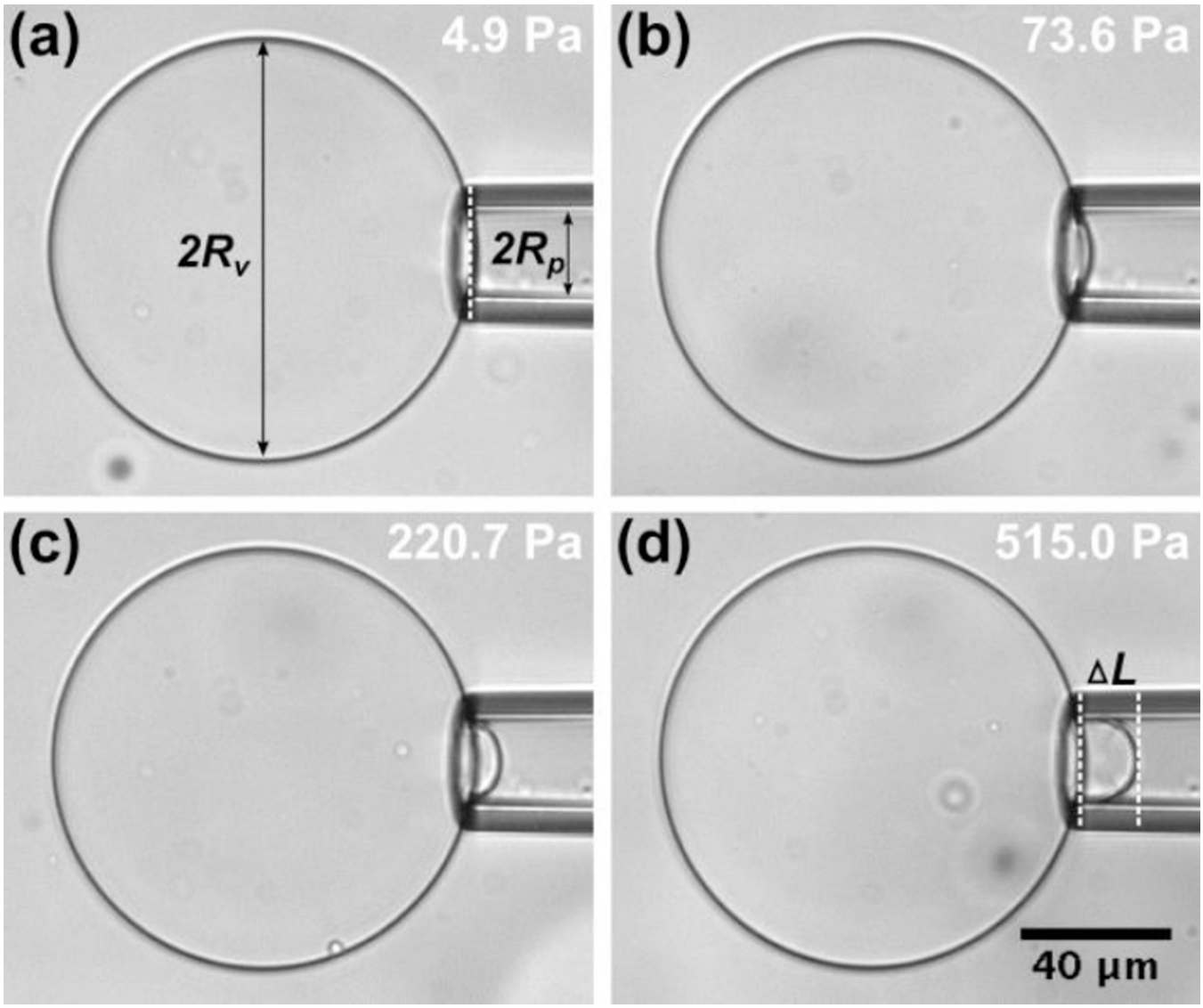

Figure 3.

Images of an asymmetric GUV (Inner leaflet: DOPC – Outer leaflet: DMPC) aspirated into a micropipette with increasing suction pressure (i.e. membrane tension) from image (a) to (d). The aspiration length at each suction pressure was recorded and compared to that in image (a), which has the lowest suction pressure, to calculate the change in aspiration length (ΔL). The measurement data of this GUV is shown in Figure 4.

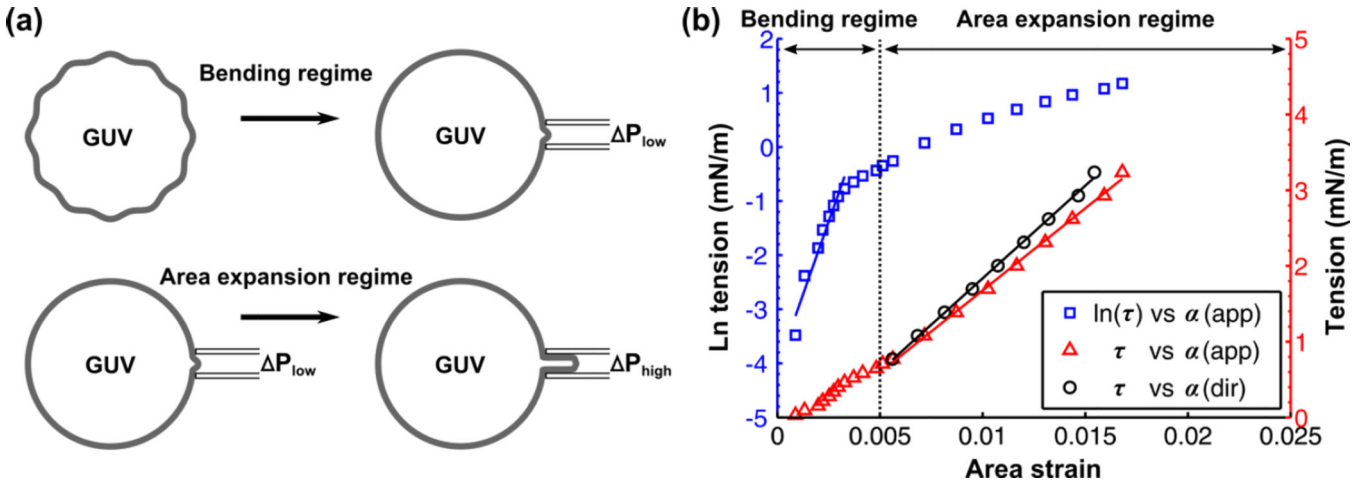

Figure 4.

(a) Schematic of tension-strain measurement on a GUV including the bending regime and area expansion regime. (b) Tension-strain measurement for an asymmetric GUV (Inner leaflet: DOPC – Outer leaflet: DMPC) made at T = 22.5°C. The blue squares denote the natural log of the tension (τ) against apparent area strain (α_{app}). A linear fit is made within the low-tension regime (<0.5 mN/m). The red triangles denote τ against α_{app}, which is nearly linear in the high-tension regime (>0.5 mN/m). Subtracting out the contribution of subvisible thermal undulations from α_{app} in the high-tension regime gives the direct area strain (α_{dir}). Thus, the re-plotted points (black squares) shift the curve to the left. The bending (κ), apparent area expansion (K_{app}), and direct area expansion (K_{dir}) moduli of this asymmetric GUV were measured to be 17.5×10^{-20} J, 217 mN/m, and 245 mN/m, respectively.

Table 1

Bending κ, direct area expansion K_{dir}, and apparent area expansion K_{app} moduli for GUV membranes as determined by micropipette aspiration measurement at T = 22.5°C

Vesicle	κ (10^{-20} J)	K_{dir} (mN/m)	K_{app} (mN/m)	*n*
DMPC	11.8 ± 1.3	173 ± 20	153 ± 17	10
DOPC	9.1 ± 1.5	210 ± 25	174 ± 20	10
DMPC/DOPC(1:1mixture)	11.2 ± 1.4	182 ± 15	159 ± 13	8
Inner: DMPC -Outer: DOPC	17.2 ± 2.5	248 ± 20	219 ± 15	8
Inner: DOPC -Outer: DMPC	16.8 ± 2.1	254 ± 19	224 ± 15	8

All values are shown as mean ± SD. n represents the number of GUVs used during measurements.